

# Optimal and fast online change point estimation in linear regression

Annika Hüselitz<sup>1</sup>, Housen Li<sup>1,2</sup>, and Axel Munk<sup>1,2</sup>

<sup>1</sup>Institute for Mathematical Stochastics, University of Göttingen

<sup>2</sup>Cluster of Excellence “Multiscale Bioimaging: from Molecular Machines to Networks of Excitable Cells” (MBExC), University of Göttingen

March 10, 2025

## Abstract

We consider the problem of sequential estimation of a single change point in a piecewise linear regression model under a Gaussian setup. We demonstrate that a certain CUSUM-type statistic attains the minimax optimal rates for localizing the change point. Our minimax analysis unveils an interesting phase transition from a *jump* (discontinuity in values) to a *kink* (change in slope). Specifically, for a jump, the minimax rate is of order  $\log(n)/n$ , whereas for a kink it scales as  $(\log(n)/n)^{1/3}$ , given that the sampling rate is of order  $1/n$ . We further introduce an algorithm for the proposed online change point detector, which requires constant computational steps and constant memory per incoming sample. Finally, the empirical performance of our method is examined on both simulated and real-world data sets. An implementation is available in the R package `FL0C` on GitHub.

Keywords: Sequential detection, minimax rate, efficient computation, Covid-19, two phase regression.

MSC2020 subject classifications: Primary 62L12, 62C20; secondary 62J20.

## 1 Introduction

Sequential change point detection, also known as online or quickest change point detection, is a classic topic in statistics with roots in ordnance testing and quality control (Shewhart, 1931; Wald, 1945; Anscombe, 1946). The primary goal is to monitor a (random) process and issue an alert when the distribution of this process deviates significantly from its historical pattern. Applications range widely, including social network monitoring (Chen, 2019), quality control in industrial processes (Amiri and Allahyari, 2012), cybersecurity (Tartakovsky et al., 2012), and seismic tremor detection (Li et al., 2018), among others.

In early work, Page (1954) introduced the celebrated CUSUM statistic based on the the log-likelihood ratio between two known distributions (representing the control and the anomaly). Lorden (1971) later established the asymptotic minimax optimality of CUSUM regarding detection delay under constraints on average run lengths. From a Bayesian perspective, the Shiryaev–Roberts procedure (Shiryaev, 1961, 1963; Roberts, 1966) is similar to CUSUM and has several optimality properties (including the aforementioned minimax optimality as well as Bayesian optimality; see e.g. Pollak, 1985; Polunchenko and Tartakovsky, 2010). Subsequent developments have expanded this scope to address unknown anomaly distributions and various models (see e.g. Siegmund, 1985, Lai, 2001, Tartakovsky, 2020 and Wang and Xie, 2024 for an overview).

Beyond statistical optimality, recent advancements emphasize computational and memory efficiency as essential *design criteria* for sequential change point analysis, especially in modern data contexts (cf. arguments in Chen et al., 2022, Section 1). This consideration becomes especially pertinent in scenarios where evaluating each

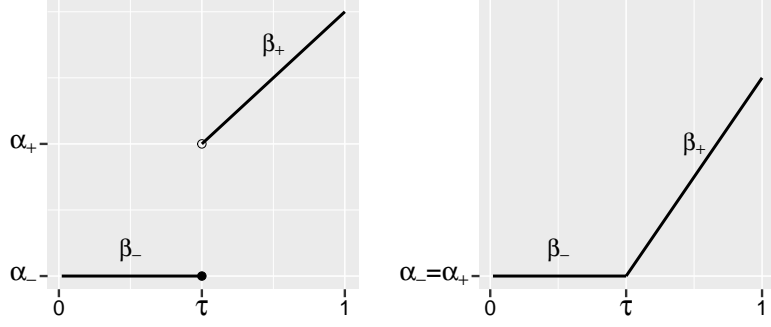


Figure 1: Sketches of some segmented linear functions  $f_\theta$  with a jump (left) and a kink (right).

candidate change point is computationally intensive (Kovács et al., 2023) and where memory resources are limited. Although computationally and memory-efficient methods are urgently needed for modern large-scale data analysis, they remain largely unexplored, with only a few exceptions (Kovács et al., 2024; Romano et al., 2023, 2024; Ward et al., 2024). A more detailed discussion of the literature from the perspective of this paper, with particular focus on minimax optimality and computational efficiency, will be presented in Section 1.2.

## 1.1 Model and main results

In this paper, we consider the sequential detection of a change in the segmented linear regression model, where observations  $X_1, \dots, X_n$  are given by

$$X_i := f_\theta\left(\frac{i}{n}\right) + \sigma\varepsilon_i, \quad i = 1, \dots, n, \quad (1a)$$

with  $\varepsilon_i \stackrel{\text{iid}}{\sim} \mathcal{N}(0, 1)$ , the standard Gaussian distribution. For simplicity, we assume that the standard deviation  $\sigma$  is known and set to 1, though it can be  $\sqrt{n}$ -consistently preestimated from data (e.g. via local differences; see e.g. Hall and Marron, 1990 and Dette et al., 1998) without affecting our results. The unknown function  $f_\theta : [0, 1] \mapsto \mathbb{R}$  is piecewise linear and takes the form of

$$f_\theta\left(\frac{i}{n}\right) := \begin{cases} \beta_- \left(\frac{i}{n} - \tau\right) + \alpha_- & \text{if } i \leq \tau, \\ \beta_+ \left(\frac{i}{n} - \tau\right) + \alpha_+ & \text{if } i > \tau, \end{cases} \quad (1b)$$

where  $\theta := (\tau, \alpha_-, \alpha_+, \beta_-, \beta_+)$  lies in the parameter space

$$\Theta_{\delta_0} := \{\theta = (\tau, \alpha_-, \alpha_+, \beta_-, \beta_+) : \delta_0 \leq \tau \leq 1 - \delta_0, \max(|\alpha_+ - \alpha_-|, |\beta_+ - \beta_-|) \geq \delta_0\}, \quad (1c)$$

for some (maybe unknown)  $\delta_0 \in (0, 1/2)$ . A key aspect of our analysis is the distinction between two types of structural changes in  $f_\theta$ : a *jump* and a *kink*. We classify a change in  $f_\theta$  as a jump if  $|\alpha_+ - \alpha_-| \geq \delta_0$ , indicating a (significant) discontinuity in function values, and as a kink if  $|\alpha_+ - \alpha_-| < \delta_0$  but  $|\beta_+ - \beta_-| \geq \delta_0$ , indicating a (significant) discontinuity in slope without a (significant) jump in values, see Figure 1. The respective parameter spaces are denoted by  $\Theta_{\delta_0}^J := \{\theta \in \Theta_{\delta_0} : |\alpha_+ - \alpha_-| \geq \delta_0\}$  for jumps and  $\Theta_{\delta_0}^K := \Theta_{\delta_0} \setminus \Theta_{\delta_0}^J$  for kinks.

Formally, we define an *online detector*  $\hat{\tau}$  as a Markov stopping time with respect to the filtration  $\{\mathcal{F}_t, 1 \leq t \leq n\}$ , where  $\mathcal{F}_t$  represents the  $\sigma$ -algebra generated by observations  $X_1, \dots, X_t$ , and let  $\mathcal{T}_n$  denote the set of all such online detectors. Following Korostelev and Korosteleva (2011, Chapter 6), we aim at achieving the convergence rate of the minimax quadratic risk of detection, as the sample size  $n$  goes to infinity, that is, the convergence rate to zero of

$$R_n^*(\delta_0) := \inf_{\hat{\tau} \in \mathcal{T}_n} \sup_{\theta = (\tau, \alpha_-, \alpha_+, \beta_-, \beta_+) \in \Theta_{\delta_0}} \mathbb{E}_\tau \left[ (\hat{\tau}_n - \tau)^2 \right],$$

Table 1: Phase transition between a jump and a kink in segmented linear regression for online (this paper) and offline (Chen, 2021) setups.

	Optimal rate in quadratic risk		Computational complexity		Memory complexity	
	online	offline	online	offline	online	offline
Jump	$\mathcal{O}(\log(n)/n)$	$\mathcal{O}(1/n)$	$\mathcal{O}(1)$ per observation	$\mathcal{O}(n^2)$	$\mathcal{O}(1)$	$\mathcal{O}(n)$
Kink	$\mathcal{O}((\log(n)/n)^{1/3})$	$\mathcal{O}((1/n)^{1/3})$	$\mathcal{O}(1)$ per observation	$\mathcal{O}(n^2)$	$\mathcal{O}(1)$	$\mathcal{O}(n)$

which balances type I (false detection) and type II (missed detection) error as

$$\mathbb{E}_\tau \left[ (\hat{\tau}_n - \tau)^2 \right] = \mathbb{E}_\tau \left[ (\hat{\tau}_n - \tau)^2 \mathbb{I}(\hat{\tau} \leq \tau) \right] + \mathbb{E}_\tau \left[ (\hat{\tau}_n - \tau)^2 \mathbb{I}(\hat{\tau} > \tau) \right].$$

This framework, rooted in in-fill asymptotics, differs slightly from conventional frameworks in sequential change point detection (see Section 1.2 below), aligning more closely with *offline* change point analysis (see e.g. Frick et al., 2014a; Niu et al., 2016; Truong et al., 2020; Cho and Kirch, 2024), where all observations are available upfront. By framing the online problem in a manner analogous to offline analysis, our approach facilitates a rigorous comparison between online and offline setups. In addition, we put emphasis simultaneously on the statistical optimality and the computation and memory efficiency. Our contributions are two folds:

- i. We introduce the Fast Limited-memory Optimal Change (FLOC) detector, which operates in constant time per observation and requires only constant memory, particularly independent of the sample size. The implementation of FLOC is provided in an R package available on GitHub under <https://github.com/AnnikaHueselitz/FLOC>.
- ii. We establish that the proposed FLOC detector achieves minimax optimal rates in quadratic risk for estimating the change point, revealing a fundamental *phase transition* between jump and kink scenarios. Specifically, the minimax rate scales as  $\mathcal{O}(\log(n)/n)$  for a jump and as  $\mathcal{O}((\log(n)/n)^{1/3})$  for a kink, underscoring the different levels of detectability between abrupt and more gradual structural changes.

This phase transition between a jump and a kink has been similarly observed in offline change point estimation in segmented linear models (Chen, 2021), see also Goldenshluger et al. (2006) for general nonparametric regression models. The literature on offline change point estimation in segmented linear models is notably extensive (see e.g. Bai and Perron, 1998, Muggeo, 2003, Frick et al., 2014b, and more recently Lee et al., 2016 and Cho et al., 2024 for high-dimensional extensions). In Table 1, we summarize the phase transition scenarios in segmented linear models, comparing online and offline setups in terms of optimal rates, computational efficiency and memory requirements. It is worth emphasizing that, unlike offline setups, where model validity is typically required globally over the whole domain of the function, our online detector FLOC is effective even with only local model validity around the change point. This flexibility makes our approach particularly well-suited for applications where model structures are reliable only within specific localized regions, as demonstrated with the real-world data set discussed in Section 4.3.

## 1.2 Related work

**Minimax optimality** We review the literature that is most pertinent to our approach from an asymptotic minimax perspective. For an infinite sequence of observations  $X_1, X_2, \dots$ , the statistical performance of an online detector  $\tilde{\tau}$ , taking values in  $\mathbb{N}$ , is often assessed by

$$\sup_{1 \leq k < \infty} D_k(\tilde{\tau}) \quad \text{subject to } \mathbb{E}[\tilde{\tau} \mid \text{no change}] \geq \gamma$$

in the asymptotic regime of  $\gamma \rightarrow \infty$ . Here,  $D_k(\cdot)$  measures the detection delay when the change occurs at  $k$ , and specific examples include

$$D_k(\tilde{\tau}) = \begin{cases} \text{ess sup } \mathbb{E}[\max(\tilde{\tau} - k + 1, 0) \mid X_1, \dots, X_{k-1}; \text{ change at } k], & \text{see Lorden (1971), or} & (2a) \\ \mathbb{E}[\tilde{\tau} - k + 1 \mid \tilde{\tau} > k; \text{ change at } k], & \text{see Pollak (1985).} & (2b) \end{cases}$$

Within this framework, Yao (1993) investigated the optimal detection of a jump, with respect to (2a), in linear regression models, and Yakir et al. (1999) studied the optimal detection of a kink with respect to (2b). One might relate such results to the model (1a)–(1c) in this paper by the correspondence of  $\hat{\tau} = \tilde{\tau}/n$  and  $n = \gamma$ .

Minimax optimality results have also been established beyond linear regression models. For instance, asymptotically optimal detection methods have been developed for mean shifts (Aue and Horváth, 2004; Yu et al., 2023), non-parametric frameworks (Chen, 2019; Horváth et al., 2021), and high-dimensional settings (Chan, 2017; Chen et al., 2022).

**Computational efficiency** Despite their statistical optimality, the aforementioned methods will be confronted with computational challenges in large-scale data sets, as both their runtime and memory usage scale linearly with the number of cumulatively observed data samples for each incoming sample. Recently, in the submodel of (1a)–(1c) with piecewise constant signals (i.e.  $\beta_- = \beta_+ = 0$ ), Romano et al. (2023) provided an efficient algorithm via functional pruning for computing the online detector by Yu et al. (2023), achieving  $\mathcal{O}(\log(t))$  computational complexity and an average memory requirement of  $\mathcal{O}(\log(t))$  at the time of  $t$  observations, for  $t = 1, \dots, n$ . Variants of it using amortized cost or information from previous iterates seem to achieve  $\mathcal{O}(1)$  computation complexity per observation, as indicated by empirical evidence (Ward et al., 2024). In addition, Chen et al. (2022) introduced an online method for a high-dimensional mean shift detection with a computational and memory complexity per observation that is independent of the number of previous samples (i.e. constant in observed sample sizes).

As an addition to the existing literature, the proposed online detector FLOC achieves constant computational and memory complexity per observation, while also attaining minimax optimal rates in terms of quadratic risk for segmented linear regression models simultaneously for jumps and kinks (see again Table 1).

### 1.3 Organization and notation

The remainder of the paper is organized as follows. In Section 2, we introduce formally the FLOC detector and establish its convergence rates in quadratic risk of estimating the change point. The lower bounds that match the derived convergence rates are given in Section 3. Section 4 examines the empirical performance of the proposed FLOC detector on both simulated and real-world data sets. All of proofs are deferred to Section 5, and Section 6 concludes the paper with a discussion.

Throughout, we denote by  $\mathbb{P}_\tau(\cdot)$  the probability measure and by  $\mathbb{E}_\tau[\cdot]$  the expectation under the model (1a)–(1c) with the true change point  $\tau$ . In particular,  $\mathbb{P}_0(\cdot)$  and  $\mathbb{E}_0[\cdot]$  refer to the case with no change (i.e.  $\tau = 0$ ). For sequences  $\{a_n\}$  and  $\{b_n\}$  of positive numbers, we use  $a_n = \mathcal{O}(b_n)$  to indicate that  $a_n \leq Cb_n$  for some finite constant  $C > 0$ .

## 2 FLOC: Statistical theory and computational complexity

In this section, we introduce the Fast Limited-memory Optimal Change (FLOC) detector, on the basis of two test statistics, one of which is used to detect a jump and the other to detect a kink. We then derive upper bounds on the quadratic risk of FLOC as well as its computational cost.

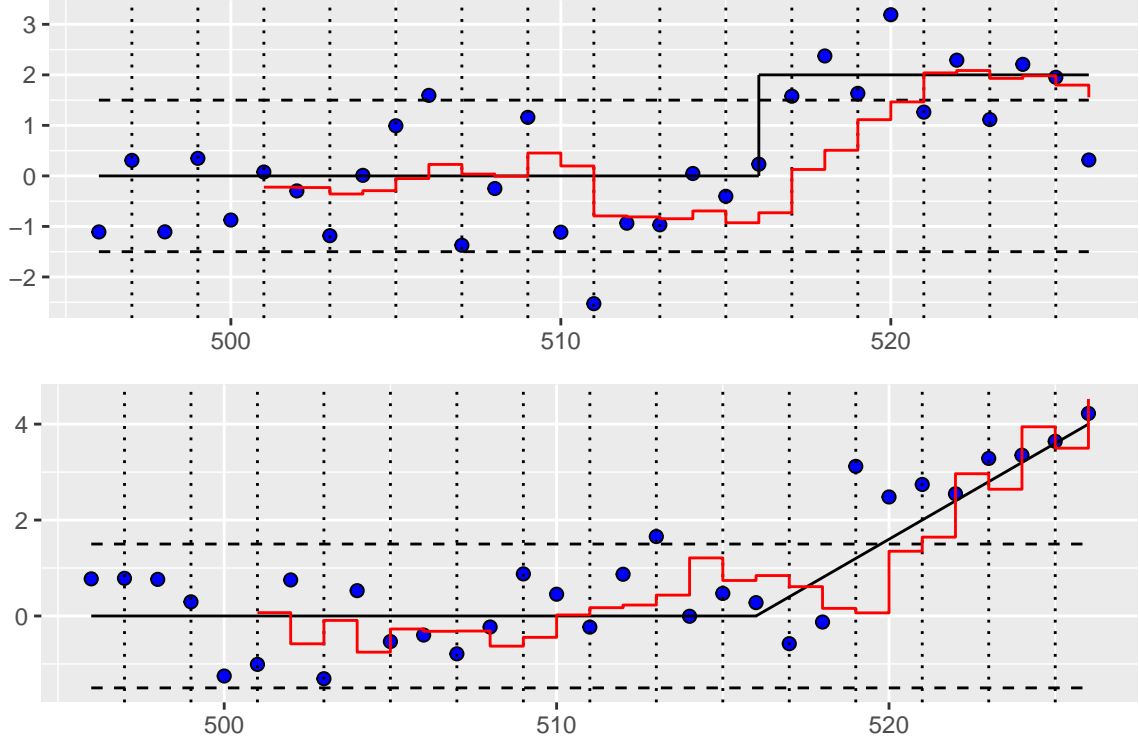


Figure 2: Simulated scenarios of a jump (upper panel) and a kink (lower panel). The black lines denote the underlying signal  $f_\theta$  with a change at  $\tau = 516/n$  and the blue dots the observations drawn under a Gaussian distribution with the signal as the mean, see (1a) and (1b). The red step functions show the values of the test statistic from FLOC. The vertical dotted lines show the observations where FLOC discards a bin; the bin sizes are  $N_J = N_K = 2$ . The pre-change signal has been estimated by the first  $k = 500$  observations. FLOC flags a change if the test statistic exceeds the threshold, with  $\rho_J = 1.5$  and  $\rho_K = 0.3$ , displayed by the dashed lines in the plot. For a jump this happens at observation 521 and for a kink at observation 521 as well. For visibility, the values of threshold and test statistic are multiplied by 5 for the kink case (lower panel).

## 2.1 Risk bounds

The idea of the online detection algorithm is to estimate the pre-change signal  $f_-$  at the beginning of the data sequence and subsequently to verify over the most recent time interval whether the data continues to adhere to the same underlying function. The detector is built upon certain test statistics, which report a change if the test statistics exceed pre-specified thresholds. For a jump we use the mean of the data on the most recent time interval as the test statistic, and for a kink we employ a weighted mean, tuned to estimate the slope of a linear function, with higher weights on more recent observations.

Consider the data sequence  $X_1, X_2, \dots, X_n$ , and let  $k, N_J, N_K \leq n$  be some natural numbers depending on  $n$ . A minimax rate optimal choice of these parameters will be specified in Theorem 1 below; The practical choice will be discussed later in Section 4.1. The function  $f_-$  is estimated using the first  $k$  data points via least squares as follows

$$\hat{f}_-\left(\frac{i}{n}\right) := \hat{\alpha} + \hat{\beta} \frac{i}{n}, \quad \text{with} \quad (\hat{\alpha}, \hat{\beta}) := \arg \min_{(\alpha, \beta) \in \mathbb{R}^2} \sum_{i=1}^k \left( \alpha + \beta \frac{i}{n} - X_i \right)^2. \quad (3a)$$

We define the *CUSUM jump test statistic* with bin size  $N_J$  as

$$J_m := \left| \frac{1}{M_J} \sum_{i=1}^{M_J} \left( X_{m-M_J+i} - \hat{f}_-\left(\frac{m-M_J+i}{n}\right) \right) \right|, \quad k < m \leq n, \quad (3b)$$

where  $M_J = 2N_J + (m \bmod N_J)$ . Similarly, the *CUSUM kink test statistic* with bin size  $N_K$  is defined as

$$K_m := \left| \frac{6}{M_K(M_K+1)(2M_K+1)} \sum_{i=1}^{M_K} i \left( X_{m-M_K+i} - \hat{f}_- \left( \frac{m-M_K+i}{n} \right) \right) \right|, \quad k < m \leq n, \quad (3c)$$

with  $M_K = 2N_K + (m \bmod N_K)$ . We introduce for some fixed thresholds  $\rho_J, \rho_K > 0$  the corresponding *detectors*  $\hat{\tau}_{J,n}$  and  $\hat{\tau}_{K,n}$  as the first time the test statistics exceed their respective thresholds, more precisely,

$$\hat{\tau}_{J,n} := \begin{cases} 1 & \text{if } J_m < \rho_J \text{ for all } m = k+1, \dots, n \\ \min(m : J_m \geq t, k < m \leq n) / n & \text{else,} \end{cases} \quad (3d)$$

for a jump and

$$\hat{\tau}_{K,n} := \begin{cases} 1 & \text{if } K_m < \rho_K \text{ for all } m = k+1, \dots, n \\ \min(m : K_m \geq t, k < m \leq n) / n & \text{else,} \end{cases} \quad (3e)$$

for a kink. Then we define the *FLOC (Fast Limited-memory Optimal Change) detector* as the minimum of the above two detectors, i.e.,

$$\hat{\tau}_n := \min(\hat{\tau}_{J,n}, \hat{\tau}_{K,n}), \quad (3f)$$

see Figure 2 for an illustration. It is straightforward to verify that the detectors  $\hat{\tau}_{J,n}$  and  $\hat{\tau}_{K,n}$ , as defined in (3d) and (3e), are Markov stopping times. As a consequence, FLOC, being the minimum of two Markov stopping times, is also a Markov stopping time, that is, FLOC is indeed an online detector (see also the proof in Section 5).

**Theorem 1.** *Assume the segmented linear regression model (1a)–(1c), and let  $\hat{f}_-$  be defined in (3a) with  $k = cn$  for some constant  $c \in (0, \delta_0)$ . Then:*

- i. *Let  $\hat{\tau}_{J,n}$  be the CUSUM jump detector in (3b) and (3d) with bin size  $N_J = 10^3 \log(n)/(2c^2)$  and threshold  $\rho_J = 4c/5$ . Then it holds for sufficiently large  $n$*

$$\sup_{\theta=(\tau, \alpha_-, \alpha_+, \beta_-, \beta_+) \in \Theta_{\delta_0}^J} \mathbb{E}_\tau \left[ \left( \frac{n}{\log n} (\hat{\tau}_{J,n} - \tau) \right)^2 \right] \leq r_J^*,$$

where  $r_J^*$  is independent of  $n$  and can be chosen as  $r_J^* = 9 \cdot 10^6 \cdot 4^{-1} \delta_0^{-4} + 1$ .

- ii. *Let  $\hat{\tau}_{K,n}$  be the CUSUM kink detector in (3c) and (3e) with bin size  $N_K = (300/c^2)^{1/3} n^{2/3} \log^{1/3}(n)$  and threshold  $\rho_K = 4c/5n$ . Then it holds for sufficiently large  $n$*

$$\sup_{\theta=(\tau, \alpha_-, \alpha_+, \beta_-, \beta_+) \in \Theta_{\delta_0}^K} \mathbb{E}_\tau \left[ \left( \frac{n^{1/3}}{\log^{1/3} n} (\hat{\tau}_{K,n} - \tau) \right)^2 \right] \leq r_K^*,$$

where  $r_K^*$  is independent of  $n$  and can be chosen as  $r_K^* = 9 \cdot 300^{2/3} \delta_0^{-4/3} + 1$ .

- iii. *For the detector FLOC defined in (3b)–(3f), both of the above rates hold for sufficiently large  $n$ .*

The idea of proof (for details see Section 5) is to characterize an event on which the detector reports a change point without false alarms and achieves a detection delay that is in the range of the considered rate; then such an event is shown to occur with a high probability. Theorem 1 provides an upper bound on the detection risk for online detectors in our model. The constants are explicit, but they are not optimized and could potentially be improved. As demonstrated later in Section 3, the rates in Theorem 1 are also achieved by lower bounds, revealing that FLOC is minimax optimal in detection of the change point.

## 2.2 Computational complexity

A pseudocode implementation of FLOC is provided in Algorithm 1. The algorithm maintains sums and weighted sums in bins of fixed size to calculate the test statistics. When the third bin is full, the first bin is discarded, and a new bin is initiated. The benefits of varying window sizes over a fixed window size become evident in the implementation of FLOC. While a constant window size achieves the same asymptotic properties, it would require storing individual observations to allow for gradual updates as the window moves. As the window size depends on  $n$ , the storage cost for a fixed window size would grow with the rate of observations. In contrast, Algorithm 1 achieves computational and memory costs of  $\mathcal{O}(1)$ , independent of the window size or the number of observation until the current time. This property is particularly advantageous for online detectors, as minimal computational and memory requirements are often considered essential design criteria (cf. Introduction).

**Proposition 2.** *For the detector FLOC as defined in (3b)–(3f), the following holds:*

- i. The computational cost is  $\mathcal{O}(1)$ .*
- ii. The storage cost is  $\mathcal{O}(1)$ .*

FLOC simultaneously monitors for both jumps and kinks by leveraging the stored sums in the computation of test statistics for both types of change. To focus on detecting only one type, we can formally set the threshold for the other to infinity. A practical challenge in Algorithm 1 is the choice of the bin sizes  $N_J, N_K$  and the thresholds  $\rho_J, \rho_K$ , as these parameters would influence the empirical performance. The parameter values used in the proof of Theorem 1 can serve as a guideline, though they are mainly tuned for their asymptotic performance. We discuss the choice of parameters in Section 4.1. The implementation can also be adapted to incorporate a known pre-change signal  $f_-$  by directly setting this in place of its estimate  $\hat{f}_-$ .

---

**Algorithm 1** FLOC: Fast Limited-memory Optimal Change detector

---

**Storage:** jump sums  $S_{J,1}, S_{J,2}, S_{J,3}$ , kink sums  $S_{K,1}, S_{K,2}, S_{K,3}$ , weighted sums  $W_1, W_2, W_3$

**Input:** latest data point  $X_t$  at time  $t$ , jump bin size  $N_J$ , kink bin size  $N_K$ , jump threshold  $\rho_J$ , kink threshold  $\rho_K$ , estimate of pre-change signal  $\hat{f}_-$

- 1: compute  $r_J \leftarrow t \bmod N_J$
  - 2: compute  $r_K \leftarrow t \bmod N_K$
  - 3: compute scaling factor  $d \leftarrow \frac{(2N_K+r_K+1)(2N_K+r_K+2)(4N_K+2r_K+3)}{6}$
  - 4: **if**  $r_J = 0$  **then**
  - 5:     update jump sums  $S_{J,1} \leftarrow S_{J,2}, S_{J,2} \leftarrow S_{J,3}, S_{J,3} \leftarrow 0$
  - 6: **end if**
  - 7: **if**  $r_K = 0$  **then**
  - 8:     update kink sums  $S_{K,1} \leftarrow S_{K,2}, S_{K,2} \leftarrow S_{K,3}, S_{K,3} \leftarrow 0$
  - 9:     update weighted sums  $W_1 \leftarrow W_2, W_2 \leftarrow W_3, W_3 \leftarrow 0$
  - 10: **end if**
  - 11: update jump sum  $S_{J,3} \leftarrow S_{J,3} + X_t - \hat{f}_-(t)$
  - 12: update kink sum  $S_{K,3} \leftarrow S_{K,3} + X_t - \hat{f}_-(t)$
  - 13: update weighted sum  $W_3 \leftarrow W_3 + (r+1)(X_t - \hat{f}_-(t))$
  - 14: compute the CUSUM jump test statistic  $J \leftarrow (S_{J,1} + S_{J,2} + S_{J,3}) / (2N_J + r_J + 1)$
  - 15: compute the CUSUM kink test statistic  $K \leftarrow (W_1 + W_2 + W_3 + N_K S_{K,2} + 2N_K S_{K,3}) / d$
  - 16: **if**  $|J| \geq \rho_J$  **then**
  - 17:     **return** jump detected
  - 18: **else if**  $|K| \geq \rho_K$  **then**
  - 19:     **return** kink detected
  - 20: **else**
  - 21:     **return** no change detected
  - 22: **end if**
-

### 3 Lower risk bounds

In this section we complement the upper bounds in the previous section with matching lower bounds, and discuss the relation to existing results in the literature.

The following theorem provides a lower bound for all online detectors (i.e. Markov stopping times).

**Theorem 3.** *Assume the segmented linear regression model (1a)–(1c). Then, there exist positive constants  $r_{*J}$  and  $r_{*K}$ , independent of  $n$ , such that:*

$$\liminf_{n \rightarrow \infty} \inf_{\hat{\tau}_n \in \mathcal{T}} \max_{\theta = (\tau, \alpha_-, \alpha_+, \beta_-, \beta_+) \in \Theta_{\delta_0}^J} \mathbb{E}_{\tau} \left[ \left( \frac{n}{\log n} (\hat{\tau}_n - \tau) \right)^2 \right] \geq r_{*J} > 0,$$

and

$$\liminf_{n \rightarrow \infty} \inf_{\hat{\tau}_n \in \mathcal{T}} \max_{\theta = (\tau, \alpha_-, \alpha_+, \beta_-, \beta_+) \in \Theta_{\delta_0}^K} \mathbb{E}_{\tau} \left[ \left( \frac{n^{1/3}}{\log^{1/3} n} (\hat{\tau}_n - \tau) \right)^2 \right] \geq r_{*K} > 0.$$

The proof of Theorem 3, detailed in Section 5, proceeds by contradiction. In the proof, we utilize a simplification by fixing the changes in jump and slope, as the lower bound will remain valid for the full parameter space. Then we consider potential change points within the unit interval, spaced in proportion to the target rate. If the specified rate were not a valid lower bound, there would be a detector such that the probability of correct detection tends to 1. However, by analyzing the likelihood ratio between two distinct change points and leveraging the property of Markov stopping times, we show that the number of possible change points grows too fast for this to occur.

In combination with Theorem 1, Theorem 3 shows that the two distinct rates for online detection of jumps and kinks are minimax optimal. These rates closely align with the offline setup, differing only in log factors (see Table 1 in the Introduction). Notably, FLOC attains the minimax optimality in detection of both jumps and kinks. For the detection of a jump, the optimal rate for the segmented linear regression model coincides with the optimal rate for the submodel with piecewise constant signal and a single jump (see e.g. Chapter 6 in Korostelev and Korosteleva, 2011). It reveals that asymptotically a change in the slope is negligible in comparison to a jump. Further, for the submodel with piecewise constant signal, Yu et al. (2023) showed a rate of order  $\log \frac{n}{\alpha}$  on the detection delay under the condition  $\mathbb{P}(\hat{\tau} < \infty \mid \text{no change}) \leq \alpha$ , which ensures that under the null hypothesis the false alarm probability of online detector is at most  $\alpha$ . The computational cost for their proposed detector scales linearly with the number of observations available at time  $t$ , and this complexity was later improved to  $\mathcal{O}(\log t)$  using functional pruning (Romano et al., 2023). In contrast, our FLOC detector, designed for a more general model, attains the same detection delay rate in this specific submodel, and requires a computational and memory costs independent of time  $t$ , see also Section 1.2.

## 4 Numerical experiments

In this section, we first introduce an empirical method for the selection of thresholds in FLOC (Algorithm 1). Then we evaluate the empirical performance of FLOC on simulated data in regard to the expected detection delay and false alarm probability. In addition, we apply FLOC to analyze the Covid-19 excess death data from the United States. The codes we use in this section are available as an R package at GitHub under <https://github.com/AnnikaHueselitz/FLOC>.

### 4.1 Tuning of thresholds

In Theorem 1, the thresholds  $\rho_J$  and  $\rho_K$  are chosen as  $4c/5$  and  $4c/5n$ , respectively, with some  $c < \delta_0$ . However, this choice might not be practical, particularly when  $\delta_0$  is unknown. In general, a higher threshold will result

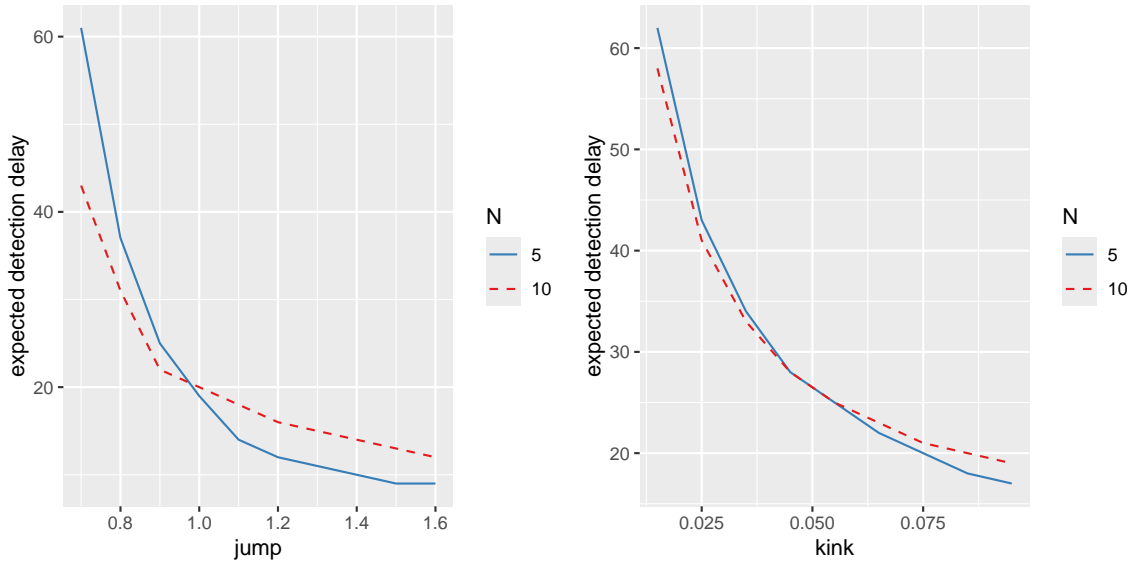


Figure 3: Expected detection delay for a true change point at observation  $\tau_0 = 500$  for bin sizes 5 (blue solid curve) and 10 (red dashed curve) for a jump (left) and a kink (right). The thresholds were tuned such that each achieves a false alarm probability of  $\mathbb{P}(\hat{\tau} \leq 1000) \approx 0.5$ . Here  $f_-$  was estimated from  $k = 500$  observations, for the threshold tuning  $r = 1000$  sets of data were generated and the estimation of the expected detection delay was done with 500 repetitions.

Table 2: Performance of FLOC (Algorithm 1) on simulated data. The thresholds  $\rho_J$  and  $\rho_K$  are tuned such that a false alarm probability (FA) of 0.5 is reached with  $k$  historical data points using 10000 repetitions. The false alarm probability and the expected detection delay, with a change point at  $\tau = k$  for jump sizes 2, 1 and 0.5 and for changes in the slope of sizes 0.5, 0.1 and 0.02 are estimated through Monte Carlo simulations with 200 repetitions.

algorithm	N	FA	k	$\rho_J$	$\rho_K$	est. FA	jump			kink		
							2	1	0.5	0.5	0.1	0.02
jump	5	1000	500	1.031	-	0.5	7	21	329	-	-	-
	10	1000	500	0.749	-	0.46	10	19	159	-	-	-
	10	1000	1000	0.658	-	0.53	9	17	63	-	-	-
	10	10000	5000	0.79	-	0.47	11	20	127	-	-	-
	15	1000	500	0.627	-	0.55	13	24	171	-	-	-
kink	5	1000	500	-	0.148	0.48	-	-	-	6	17	52
	10	1000	500	-	0.058	0.51	-	-	-	8	18	47
	10	1000	1000	-	0.051	0.54	-	-	-	7	17	44
	10	10000	5000	-	0.062	0.52	-	-	-	9	19	52
	15	1000	500	-	0.033	0.46	-	-	-	8	18	49
both	5	1000	500	1.071	0.15	0.5	6	17	352	6	16	49
	10	1000	500	0.781	0.06	0.54	9	19	221	8	19	47
	10	1000	1000	0.687	0.05	0.46	8	15	73	8	17	43
	10	10000	5000	0.818	0.06	0.46	10	20	133	9	20	52
	15	1000	500	0.651	0.03	0.54	11	22	192	8	18	48

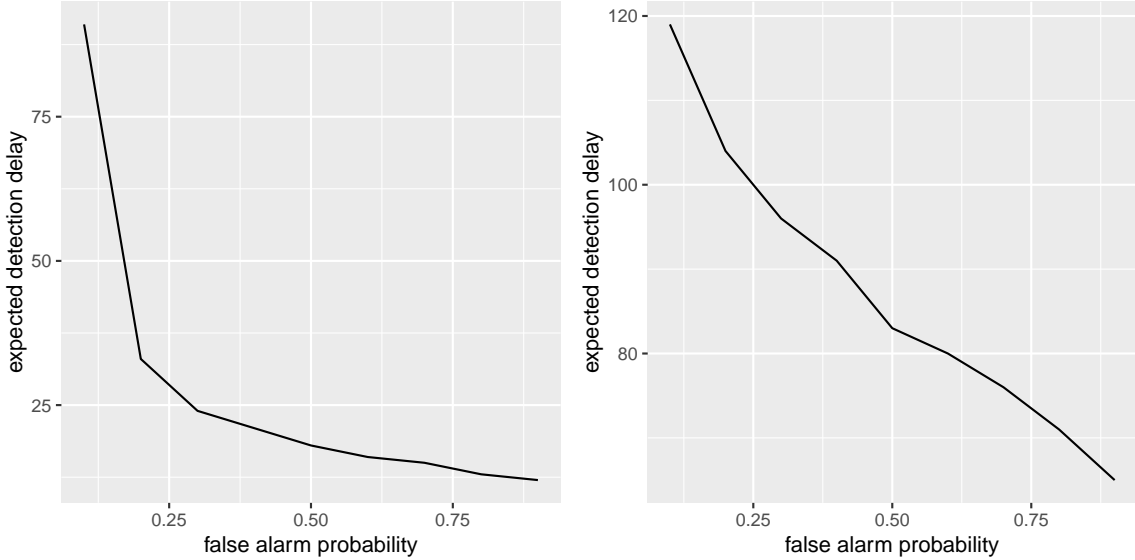


Figure 4: Comparison of the type I error of a false alarm probability for  $\tau = 1000$  and the type II error of the expected detection delay with a change point at  $\tau = 500$ , for the jump algorithm (left) and the kink algorithm (right). In both plots, the bin size is  $N_J = N_K = 5$  and  $f_-$  is estimated with  $k = 500$  observations, the threshold tuning was made with  $r = 5000$  repetitions and the expected detection delay was estimated with 200 repetitions. The jump size for the detection delay is 1 and the change in slope is 0.01.

in a decrease in the type I error and an increase in the type II error. The type I error is typically measured by the *false alarm probability*  $\mathbb{P}_\tau(\hat{\tau} \leq \tau)$ , which is the probability that a false alarm occurs, or by the *average run length* under the null hypothesis  $\mathbb{E}_0[\hat{\tau}]$ , which is the expected run length if no change occurs. The type II error is often measured by the *expected detection delay*  $\mathbb{E}_\tau[(\hat{\tau} - \tau)_+]$ . In practice, thresholds can be tuned to control the type I error at a rate  $\eta$ , specified by the practitioners, in terms of e.g. the false alarm probability  $\mathbb{P}_\tau(\hat{\tau} \leq \tau)$ . The task of selecting a threshold then reduces to identifying the smallest value such that  $\mathbb{P}_\tau(\hat{\tau} \leq \tau) \leq \eta$  for some fixed  $\tau$ . This approach is feasible because the false alarm probability of FLOC depends primarily on the position of the change point of the signal and not on the slopes or intercepts of the segments. Note that it also depends on the amount of historical data available. To estimate the thresholds  $\rho_J$  and  $\rho_K$  for fixed bin sizes  $N_J$  and  $N_K$  with  $k$  historical observations, such that  $\mathbb{P}_\tau(\hat{\tau} \leq \tau) \approx \eta$  for  $\tau \in \mathbb{N}$  and  $\eta \in (0, 1)$ , we generate data  $X_1^{(m)}, \dots, X_{\tau_0+k}^{(m)}$  for  $1 \leq m \leq r$  under the null hypothesis, and then compute the maximum statistics  $M_{J,m} := \max_{1 \leq i < \tau} J_i^{(m)}$  for jump detection and  $M_{K,m} := \max_{1 \leq i < \tau} K_i^{(m)}$  for kink detection. For the component of jump detection in FLOC (or equivalently, setting the kink threshold as infinity), we select the jump threshold  $\rho_J$  as the  $(1 - \eta)$ -quantile of  $\{M_{J,m} : 1 \leq m \leq r\}$ , since  $1 - \eta = \mathbb{P}_\tau(M_{J,m} < t) = \mathbb{P}_\tau(\hat{\tau} > \tau) = 1 - \mathbb{P}_\tau(\hat{\tau} \leq \tau)$ . A similar procedure applies to the kink detection component. When the algorithm runs for both change types simultaneously, thresholds can be chosen to ensure  $\mathbb{P}_\tau(\hat{\tau}_J \leq \tau) \approx \mathbb{P}_\tau(\hat{\tau}_K \leq \tau)$ . This is achieved by consider the respective quantiles of  $M_{J,m}$  and  $M_{K,m}$  at the same level and selecting the highest level that satisfies  $\mathbb{P}_\tau(M_{J,m} < \rho_J, M_{K,m} < \rho_J) \leq \eta$ .

## 4.2 Simulated data

Figure 3 compares the performance of FLOC with bin sizes  $N_J = N_K = 5$  and  $N_J = N_K = 10$ . All thresholds are tuned according to Section 4.1 to achieve a false alarm probability of  $\mathbb{P}(\hat{\tau} \leq 1000) \approx 0.5$ . Both configurations demonstrated that larger changes could be detected with shorter expected detection delays compared to smaller changes. The larger bin size ( $N_J = N_K = 10$ ) performs better for detecting smaller jump sizes (less than 1) and smaller changes in slope (less than 0.05). Conversely, the smaller bin size ( $N_J = N_K = 5$ ) performs better for detecting larger changes (jump sizes greater than 1 and slope changes greater than 0.05). Notably, this difference occurs in the regime where the expected detection delay is between 20 and 30. In such cases, the larger window size (10) needs to encompass nearly the entire change point to detect the change effectively.

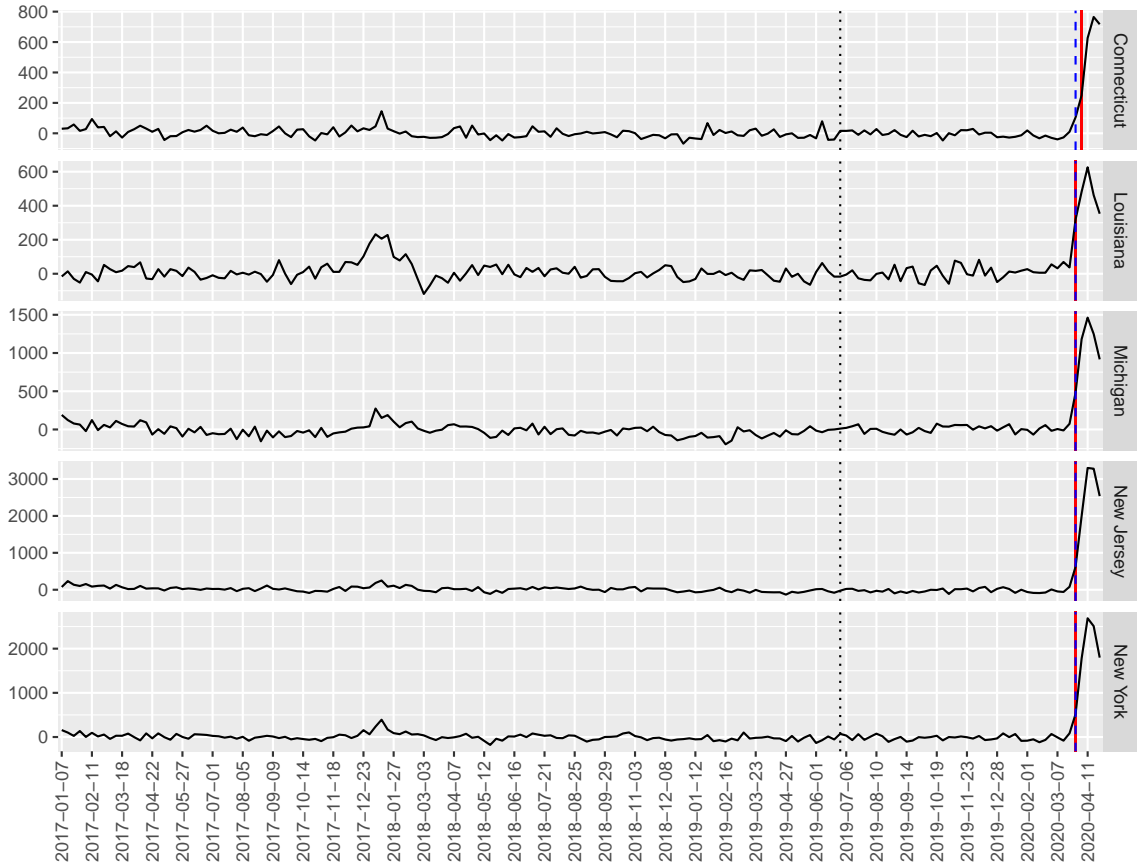


Figure 5: Excess death data in the states identified as significant by `ocd_CI` (Chen et al., 2024). The blue dashed line marks the change detected by `ocd_CI`, while red lines indicate changes detected by FLOC. The data up to the dotted line (2020-06-30) serves as historical data for both algorithms.

To evaluate the statistical performance of the algorithms, we assess the type I error by the false alarm probability and the type II error by the expected detection delay. As expected, reducing the type I error will increase the type II error and vice versa. Figure 4 illustrates the relationship between the false alarm probability and the expected detection delay, when the bin size and change magnitude are fixed.

Table 2 summarizes the performance of the algorithms for different bin sizes and type I error bounds. The results indicate that smaller bin sizes lead to better performance in detecting larger changes, while larger window sizes are more effective for detecting smaller changes. Additionally, the table confirms that the threshold tuning approach described in Section 4.1 is effective, producing the the desired false alarm probabilities.

### 4.3 Real data

To evaluate the empirical performance of FLOC on real-world data, we analyze excess mortality data from the CDC website [https://www.cdc.gov/nchs/nvss/vsrr/covid19/excess\\_deaths.htm](https://www.cdc.gov/nchs/nvss/vsrr/covid19/excess_deaths.htm). This data set consists of estimates of excess deaths in the United States from the beginning of 2017 through September of 2023 by states (see Figures 5 and 6), which were calculated based on weekly counts of deaths using Farrington surveillance algorithms (Noufaily et al., 2013, see the CDC website for further details). For our analysis, we treat the data through the end of June 2019 as historical data, and standardize the entire data set with the mean and the standard deviation of the historical period. The primary objective of this analysis is to study the impact of Covid-19. This data set was also used by Chen et al. (2024) to demonstrate the effectiveness of their online algorithm `ocd_CI`, which detects changes in high-dimensional means. We thus include `ocd_CI` as a baseline for comparison with FLOC.

The increase in excess deaths to the onset of Covid-19 appears to exhibit a gradual change in slope, rather



Figure 6: Standardized excess death data for Arkansas, Kentucky, Virginia, and the United States (pooled data). The red step function represents the test statistic values of FLOC, scaled by a factor of 4 for visibility. The horizontal dashed line marks the detection threshold, and the vertical red line indicates the detected change in slope.

than abrupt changes in values (see again Figures 5 and 6). Therefore, we apply only the kink component of the FLOC algorithm by setting the jump threshold as infinity. We choose a bin size of  $N_k = 2$  weeks, and tune the (kink) threshold  $\rho_K = 0.738$  to maintain a false alarm probability of approximately 0.01 on the remaining data. The FLOC algorithm is applied individually to each state as well as to the pooled data for the United States. In contrast, the `ocd_CI` method is applied to the entire data set, identifying a common change across all states and reporting a subset of states where this change occurs.

Figure 5 shows the detection results of FLOC and `ocd_CI` across the five states identified by `ocd_CI` as having significant changes. In four of these five states (New York, New Jersey, Louisiana and Michigan), both algorithms detect changes during the week ending March 28, 2020. For the fifth state (Connecticut), FLOC identifies a change in the week ending April 4, 2020, which slightly differs from `ocd_CI` (March 28, 2020). These detected changes align well with the timeline of Covid-19 outbreak in the United States as documented by the CDC (at <https://www.cdc.gov/museum/timeline/covid19.html>). In addition to these states, FLOC identifies changes in regions with a more moderate rise in excess deaths, where `ocd_CI` does not detect any changes. For example, FLOC detects changes in Virginia during the week ending April 11, 2020, in Arkansas during the week ending July 4, 2020, and in Kentucky during the week ending May 23, 2020. Further, FLOC detects a change in the pooled data for the United States in the week ending March 28, 2020. Figure 6 presents a selection of the excess death curves and the corresponding changes detected by FLOC.

While FLOC yields insightful results on this data set, we acknowledge potential violations of the model assumptions in Section 1.1. For instance, the data exhibits positive correlation, as shown by the autocorrelation function (ACF) plots in Figure 7. We note that `ocd_CD` also does not take the serial dependency into account (see Chen et al., 2024). Furthermore, the underlying signal adheres to a kink-like structure only locally around the change points. A comprehensive analysis that incorporates the dependence structure of the data is beyond

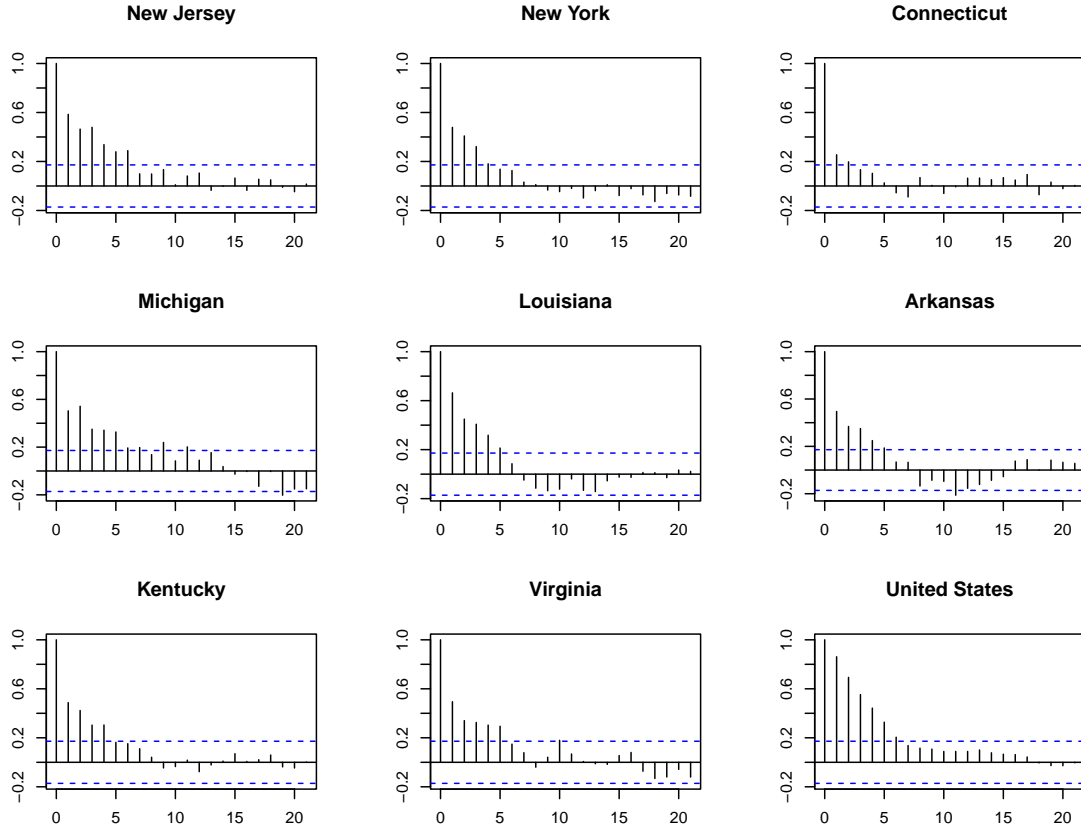


Figure 7: ACF plots showing the autocorrelation of excess death data (up to June 30, 2020) at various time lags for selected states and the pooled data for the United States.

the scope of this paper and warrants further investigation.

## 5 Proofs

*Proof of Theorem 1.* The proof is divided in two parts. In the first part we show the upper bound for a jump at the change point and in the second part the upper bound for a kink at the change point. The statement for the FLOC algorithm then follows naturally. We will denote by  $f_-(\cdot) := \beta_-(\cdot - \tau) + \alpha_-$  and  $f_+(\cdot) := \beta_+(\cdot - \tau) + \alpha_+$  the linear functions, which correspond to the two segments of  $f_{\theta_0}$ .

**For a jump** Now we assume that a jump at the change point occurs, namely,  $|\alpha_+ - \alpha_-| \geq \delta_0$ , for some  $\delta_0 > 0$ . We take (3d) as our detector. For this, we set  $N_J := b \log n$ , with some  $b$  independent of  $n$ , which we will specify later on. We fix some  $c \in (0, 1)$  and take the threshold as  $\rho_J = 4c/5$ . We set the number of data points to estimate  $f_-$  as  $k = cn$ . Recall that  $N_J$  is the number of observations in a bin and set  $M_J = 2N_J + (m \bmod N_J)$  as the window size at time  $m$ , on which we calculate the test statistics. Here we suppress the dependency of  $M_J$  on  $m$ , as it is important for the storage complexity, but for this proof we only need that  $2N_J \leq M_J < 3N_J$ . For notational ease, we assume that both are integers, and otherwise only small adjustments would be needed. We write only  $N_J = N$  and  $M_J = M$  for the jump part.

The detector defined in (3d) is a stopping time, because  $\{\hat{\tau}_{J,n} = s/n\} = \{J_s \geq \rho_J, J_m < \rho_J, k \leq m \leq s-1\}$ . Note that  $\{\hat{\tau}_{J,n} = s/n\}$  is determined by  $J_1, \dots, J_s$ , which are determined by  $X_1, \dots, X_s$  and therefore independent of  $X_{s+1}, \dots, X_n$ . Thus,  $\{\hat{\tau}_{J,n} = s/n\}$  is  $\mathcal{F}_s$ -measurable.

Denote by  $\tau_0$  the time of the true change point. Then, for  $m < n\tau_0$ , i.e. the test statistics before the true

change point

$$J_m = \left| \frac{1}{M} \sum_{i=1}^M \varepsilon_{m-M+i} + \frac{1}{M} \sum_{i=1}^M \left( f_- \left( \frac{m-M+i}{n} \right) - \hat{f}_- \left( \frac{m-M+i}{n} \right) \right) \right|$$

$$\leq \left| \frac{1}{M} \sum_{i=1}^M \varepsilon_{m-M+i} \right| \tag{4a}$$

$$+ \left| \frac{1}{M} \sum_{i=1}^M \left( f_- \left( \frac{m-M+i}{n} \right) - \hat{f}_- \left( \frac{m-M+i}{n} \right) \right) \right|. \tag{4b}$$

And for  $m_0 = \lceil n\tau_0 \rceil + 3N - 1$ , i.e. the test statistics after the true change point,

$$J_{m_0} = \left| \frac{1}{M} \sum_{i=1}^M \varepsilon_{m_0-M+i} + \frac{1}{M} \sum_{i=1}^M \left( f_+ \left( \frac{m_0-M+i}{n} \right) - \hat{f}_- \left( \frac{m_0-M+i}{n} \right) \right) \right|$$

$$= \left| \frac{1}{M} \sum_{i=1}^M \varepsilon_{m_0-M+i} + \frac{1}{M} \sum_{i=1}^M \left( f_- \left( \frac{m_0-M+i}{n} \right) - \hat{f}_- \left( \frac{m_0-M+i}{n} \right) \right) \right.$$

$$\quad \left. + \frac{1}{M} \sum_{i=1}^M \left( f_+ \left( \frac{m_0-M+i}{n} \right) - f_- \left( \frac{m_0-M+i}{n} \right) \right) \right|$$

$$\geq \left| \frac{1}{M} \sum_{i=1}^M \left( f_+ \left( \frac{m_0-M+i}{n} \right) - f_- \left( \frac{m_0-M+i}{n} \right) \right) \right| \tag{5a}$$

$$- \left| \frac{1}{M} \sum_{i=1}^M \varepsilon_{m_0-M+i} \right| \tag{5b}$$

$$- \left| \frac{1}{M} \sum_{i=1}^M \left( f_- \left( \frac{m_0-M+i}{n} \right) - \hat{f}_- \left( \frac{m_0-M+i}{n} \right) \right) \right|. \tag{5c}$$

For the summand (5a), we have, because  $m_0 - M - n\tau_0 \leq 3N - M \leq N$ ,

$$\left| \frac{1}{M} \sum_{i=1}^M \left( f_+ \left( \frac{m_0-M+i}{n} \right) - f_- \left( \frac{m_0-M+i}{n} \right) \right) \right|$$

$$= \left| \frac{1}{M} \sum_{i=1}^M \left( (\beta_+ - \beta_-) \left( \frac{m_0-M+i}{n} - \tau_0 \right) + \alpha_+ - \alpha_- \right) \right|$$

$$\geq |\alpha_+ - \alpha_-| - |\beta_+ - \beta_-| \frac{1}{M} \sum_{i=1}^M \left( \frac{m_0-M+i}{n} - \tau_0 \right)$$

$$\geq |\alpha_+ - \alpha_-| - |\beta_+ - \beta_-| \frac{1}{M} \sum_{i=1}^M \frac{N+i}{n} = |\alpha_+ - \alpha_-| - |\beta_+ - \beta_-| \frac{2N + M(M+1)}{2n}$$

$$> c,$$

for  $c < |\alpha_+ - \alpha_-|$  and  $n$  large enough. Such a  $c$  exists as  $0 < \delta_0 \leq |\alpha_+ - \alpha_-|$ .

We set  $Z_m := \sum_{i=1}^M \varepsilon_{m-M+i} / \sqrt{M} \sim \mathcal{N}(0, 1)$  and define the event

$$\mathcal{A} := \left\{ \max_{k < m \leq n} |Z_m| < \sqrt{10 \log n}, \max_{1 \leq i \leq n} \left| f_- \left( \frac{i}{n} \right) - \hat{f}_- \left( \frac{i}{n} \right) \right| < \frac{c}{10} \right\}.$$

For the summands (4a) and (5b) under the event  $\mathcal{A}$  with  $b = 10^3/2c^2$  it holds

$$\left| \frac{1}{M} \sum_{i=1}^M \varepsilon_{m-M+i} \right| \leq \max_{k < m \leq n} \left| \frac{Z_m}{\sqrt{M}} \right| < \frac{\sqrt{10 \log n}}{\sqrt{M}} \leq \sqrt{\frac{10 \log n}{2N}} = \sqrt{\frac{10 \log n}{2b \log n}} = \sqrt{\frac{10c^2}{10^3}} = \frac{c}{10}. \tag{6}$$

For the parts (4b) and (5c) under the event  $\mathcal{A}$  it holds

$$\begin{aligned} & \left| \frac{1}{M} \sum_{i=1}^M \left( f_- \left( \frac{m-M+i}{n} \right) - \hat{f}_- \left( \frac{m-M+i}{n} \right) \right) \right| \\ & \leq \frac{1}{M} \sum_{i=1}^M \left| f_- \left( \frac{m-M+i}{n} \right) - \hat{f}_- \left( \frac{m-M+i}{n} \right) \right| < \frac{c}{10}. \end{aligned}$$

Let  $c < \delta_0$ . Under the event  $\mathcal{A}$ , for  $m < n\tau_0$ , it holds that  $J_m < c/10 + c/10 < 4c/5 = \rho_J$  and  $J_{m_0} > c - c/10 - c/10 = 4c/5 = \rho_J$ , and thus,  $n\tau_0 \leq n\hat{\tau}_{J,n} \leq m_0$ .

For  $Z \sim \mathcal{N}(0, 1)$  and  $y > 1$ , using Mill's ratio, we obtain

$$\mathbb{P}(|Z| \geq y) = 2\mathbb{P}(Z \geq y) \leq \frac{2}{\sqrt{2\pi}y^2} \exp\left\{-\frac{y^2}{2}\right\} \leq \exp\left\{-\frac{y^2}{2}\right\}, \quad (7)$$

and therefore using the union bound

$$\mathbb{P}_{\tau_0} \left( \max_{k < m \leq n} |Z_m| \geq y \right) \leq n \exp\left\{-\frac{y^2}{2}\right\}. \quad (8)$$

When we set  $y = \sqrt{10 \log n} > 1$ , we have for  $n$  large enough

$$\mathbb{P}_{\tau_0} \left( \max_{k < m \leq n} |Z_m| \geq \sqrt{10 \log n} \right) \leq n \exp\{-5 \log n\} = n^{-4}. \quad (9)$$

We can use Korostelev and Korosteleva (2011, Theorem 7.5) to show that

$$\hat{\alpha} \sim \mathcal{N} \left( \alpha_- - \beta_- \tau_0, \frac{4cn + 2}{c^2 n^2 - cn} \right) \text{ and } \hat{\beta} \sim \mathcal{N} \left( \beta_-, \frac{12n}{c^3 n^2 - c} \right).$$

Define

$$Z_\alpha = (\alpha_- - \beta_- \tau_0 - \hat{\alpha}) \sqrt{\frac{c^2 n^2 - cn}{4cn + 2}} \sim \mathcal{N}(0, 1) \text{ and } Z_\beta = (\beta_- - \hat{\beta}) \sqrt{\frac{c^3 n^2 - c}{12n}} \sim \mathcal{N}(0, 1).$$

Now we can use the inequality (7) to obtain for any  $\epsilon > 0$

$$\begin{aligned} & \mathbb{P} \left( \max_{1 \leq i \leq n} \left| f_- \left( \frac{i}{n} \right) - \hat{f}_- \left( \frac{i}{n} \right) \right| \geq \epsilon \right) \leq \mathbb{P} \left( \left\{ |f_-(0) - \hat{f}_-(0)| \geq \epsilon \right\} \cup \left\{ |f_-(1) - \hat{f}_-(1)| \geq \epsilon \right\} \right) \\ & = \mathbb{P} \left( \left\{ |\alpha_- - \beta_- \tau_0 - \hat{\alpha}| \geq \epsilon \right\} \cup \left\{ |\alpha_- + \beta_- (1 - \tau_0) - \hat{\alpha} - \hat{\beta}| \geq \epsilon \right\} \right) \\ & \leq \mathbb{P} \left( \left\{ |\alpha_- - \beta_- \tau_0 - \hat{\alpha}| \geq \epsilon \right\} \cup \left\{ |\beta_- - \hat{\beta}| \geq \frac{\epsilon}{2} \right\} \right) \\ & \leq \mathbb{P}(|\alpha_- - \beta_- \tau_0 - \hat{\alpha}| \geq \epsilon) + \mathbb{P} \left( |\beta_- - \hat{\beta}| \geq \frac{\epsilon}{2} \right) \\ & = \mathbb{P} \left( |Z_\alpha| \geq \epsilon \sqrt{\frac{c^2 n^2 - cn}{4cn + 2}} \right) + \mathbb{P} \left( |Z_\beta| \geq \frac{\epsilon}{2} \sqrt{\frac{c^3 n^2 - c}{12n}} \right) \\ & \leq \exp \left\{ -\frac{\epsilon^2 (c^2 n^2 - cn)}{8cn + 4} \right\} + \exp \left\{ -\frac{\epsilon^2 (c^3 n^2 - c)}{96n} \right\}, \end{aligned} \quad (10)$$

and therefore

$$\begin{aligned} & \mathbb{P} \left( \max_{1 \leq i \leq n} \left| f_- \left( \frac{i}{n} \right) - \hat{f}_- \left( \frac{i}{n} \right) \right| \geq \frac{c}{10} \right) \leq \exp \left\{ -\frac{c^2 (c^2 n^2 - cn)}{800cn + 4} \right\} + \exp \left\{ -\frac{c^2 (c^3 n^2 - c)}{9600n} \right\} \\ & \ll n^{-4}. \end{aligned} \quad (11)$$

We can combine (9) and (11) to get

$$\mathbb{P}(\mathcal{A}^c) \leq \mathbb{P}\left(\max_{1 \leq m \leq M} |Z_m| \geq y\right) + \mathbb{P}\left(\max_{1 \leq i \leq n} \left|f_-\left(\frac{i}{n}\right) - \hat{f}_-\left(\frac{i}{n}\right)\right| \geq \frac{c}{10}\right) \leq n^{-4}.$$

To summarize, we have shown that under the event  $\mathcal{A}$ , it holds that  $0 \leq \hat{\tau}_{J,n} - \tau_0 \leq 3N/n$  and  $\mathbb{P}(\mathcal{A}^c) \leq n^{-4}$ . Thus, since  $1/n^2 \log^2 n < 1$  for  $n \geq 2$ ,

$$\begin{aligned} & \max_{\theta_0 \in \Theta^J} \mathbb{E}_{\tau_0} \left[ \left( \frac{n}{\log n} (\hat{\tau}_{J,n} - \tau_0) \right)^2 \right] \\ &= \max_{\theta_0 \in \Theta^J} \left( \mathbb{E}_{\tau_0} \left[ \left( \frac{n}{\log n} (\hat{\tau}_{J,n} - \tau_0) \right)^2 \mathbb{I}(\mathcal{A}) \right] + \mathbb{E}_{\tau_0} \left[ \left( \frac{n}{\log n} (\hat{\tau}_{J,n} - \tau_0) \right)^2 \mathbb{I}(\mathcal{A}^c) \right] \right) \\ &\leq \max_{\theta_0 \in \Theta^J} \left( \mathbb{E}_{\tau_0} \left[ \left( \frac{3N}{\log n} \right)^2 \mathbb{I}(\mathcal{A}) \right] + \mathbb{E}_{\tau_0} \left[ \left( \frac{n}{\log n} \right)^2 \mathbb{I}(\mathcal{A}^c) \right] \right) \\ &\leq \left( \frac{3N}{\log n} \right)^2 + \left( \frac{n}{\log n} \right)^2 n^{-4} \leq 9b^2 + 1 = 9\frac{10^6}{4c^4} + 1. \end{aligned}$$

Therefore, the statement about a jump is true with  $r_J^* = 9(10^6/4\delta_0^4) + 1$ .

**For a kink** In the case of a kink, we assume that  $|\beta_+ - \beta_-| \geq \delta_0$  and  $|\alpha_+ - \alpha_-| < \delta_0$ . Here we set  $N := bn^{2/3} \log^{1/3} n$ , assumed to be an integer, with  $b$  positive and independent of  $n$  and  $M := 2N + (m \bmod N)$ . We set the threshold as  $\rho_K = 4c/5n$  for some fixed  $c > 0$ . We scale our test statistic by  $d_M := M(M+1)(2M+1)/6$ . For  $m < n\tau_0$ , it holds

$$\begin{aligned} K_m &= \left| \frac{1}{d_M} \sum_{i=1}^M i \varepsilon_{m-M+i} + \frac{1}{d_M} \sum_{i=1}^M i \left( f_-\left(\frac{m-M+i}{n}\right) - \hat{f}_-\left(\frac{m-M+i}{n}\right) \right) \right| \\ &\leq \left| \frac{1}{d_M} \sum_{i=1}^M i \varepsilon_{m-M+i} \right| \end{aligned} \tag{12a}$$

$$+ \left| \frac{1}{d_M} \sum_{i=1}^M i \left( f_-\left(\frac{m-M+i}{n}\right) - \hat{f}_-\left(\frac{m-M+i}{n}\right) \right) \right|. \tag{12b}$$

And for  $m_0 := \lceil n\tau_0 \rceil + 3N - 1$ , we get

$$\begin{aligned} K_{m_0} &= \left| \frac{1}{d_M} \sum_{i=1}^M i \varepsilon_{m_0-M+i} + \frac{1}{d_M} \sum_{i=1}^M i \left( f_+\left(\frac{m_0-M+i}{n}\right) - \hat{f}_-\left(\frac{m_0-M+i}{n}\right) \right) \right| \\ &= \left| \frac{1}{d_M} \sum_{i=1}^M i \varepsilon_{m_0-M+i} + \frac{1}{d_M} \sum_{i=1}^M i \left( f_-\left(\frac{m_0-M+i}{n}\right) - \hat{f}_-\left(\frac{m_0-M+i}{n}\right) \right) \right. \\ &\quad \left. + \frac{1}{d_M} \sum_{i=1}^M i \left( f_+\left(\frac{m_0-M+i}{n}\right) - f_-\left(\frac{m_0-M+i}{n}\right) \right) \right| \\ &\geq \left| \frac{1}{d_M} \sum_{i=1}^M i \left( f_+\left(\frac{m_0-M+i}{n}\right) - f_-\left(\frac{m_0-M+i}{n}\right) \right) \right| \end{aligned} \tag{13a}$$

$$- \left| \frac{1}{d_M} \sum_{i=1}^M i \varepsilon_{m_0-M+i} \right| \tag{13b}$$

$$- \left| \frac{1}{d_M} \sum_{i=1}^M i \left( f_-\left(\frac{m_0-M+i}{n}\right) - \hat{f}_-\left(\frac{m_0-M+i}{n}\right) \right) \right|. \tag{13c}$$

As there is a kink and  $m_0 - M - n\tau_0 \geq 0$ , we get for the summand (13a), in the case of  $|\alpha_+ - \alpha_-| = 0$ ,

$$\begin{aligned} & \left| \frac{1}{d_M} \sum_{i=1}^M i \left( f_+ \left( \frac{m_0 - M + i}{n} \right) - f_- \left( \frac{m_0 - M + i}{n} \right) \right) \right| \\ &= \left| \frac{1}{d_M} \sum_{i=1}^M i \left( (\beta_+ - \beta_-) \left( \frac{m_0 - M + i}{n} - \tau_0 \right) \right) \right| \\ &\geq \frac{|\beta_+ - \beta_-|}{d_M} \sum_{i=1}^M i \left( \frac{m_0 - M + i}{n} - \tau_0 \right) \geq \frac{|\beta_+ - \beta_-|}{d_M n} \sum_{i=1}^M i^2 > \frac{c}{n}, \end{aligned}$$

for  $|\beta_+ - \beta_-| > c$ . In the case of  $|\alpha_+ - \alpha_-| > 0$ , as  $m_0 - M - n\tau_0 \leq N$ , the summand (13a) can be bounded as follows

$$\begin{aligned} & \left| \frac{1}{d_M} \sum_{i=1}^M i \left( f_+ \left( \frac{m_0 - M + i}{n} \right) - f_- \left( \frac{m_0 - M + i}{n} \right) \right) \right| \\ &= \left| \frac{1}{d_M} \sum_{i=1}^M i \left( (\beta_+ - \beta_-) \left( \frac{m_0 - M + i}{n} - \tau_0 \right) + \alpha_+ - \alpha_- \right) \right| \\ &\geq \frac{|\alpha_+ - \alpha_-|}{d_M} \sum_{i=1}^M i - \frac{|\beta_+ - \beta_-|}{d_M} \sum_{i=1}^M i \left( \frac{m_0 - M + i}{n} - \tau_0 \right) \\ &\geq \frac{3|\alpha_+ - \alpha_-|}{2M+1} - \frac{|\beta_+ - \beta_-|}{d_M n} \sum_{i=1}^M i(i+N) = \frac{3|\alpha_+ - \alpha_-|}{2M+1} - \frac{|\beta_+ - \beta_-|}{n} \left( 1 + \frac{3N}{2M+1} \right) \\ &> \frac{c}{n}, \end{aligned}$$

for  $n$  large enough. Set  $Z_m := (1/\sqrt{d_M}) \sum_{i=1}^M i \varepsilon_{m-M+i}$  for  $m = k+1, \dots, n$  standard normal distributed. Next we define the event

$$\mathcal{A} := \left\{ \max_{k < m \leq n} |Z_m| < \sqrt{8 \log n}, \max_{1 \leq i \leq n} \left| f_- \left( \frac{i}{n} \right) - \hat{f}_- \left( \frac{i}{n} \right) \right| < \frac{c(2M+1)}{30n} \right\}.$$

For the parts (12a) and (13b), it holds under the event  $\mathcal{A}$  with  $b = (300/c^2)^{1/3}$  that

$$\begin{aligned} \left| \frac{1}{d_M} \sum_{i=1}^M i \varepsilon_{m-M+i} \right| &\leq \max_{k < m \leq n} \frac{1}{\sqrt{d_M}} |Z_m| < \frac{\sqrt{8 \log n}}{\sqrt{d_M}} = \sqrt{\frac{48 \log n}{2M^3 + 3M^2 + M}} \leq \sqrt{\frac{24 \log n}{(2N)^3}} \\ &= \sqrt{\frac{3 \log n}{b^3 n^2 \log n}} = \frac{c}{10n}. \end{aligned}$$

And for the parts (12b) and (13c), it holds under the event  $\mathcal{A}$  that

$$\begin{aligned} \left| \frac{1}{d_M} \sum_{i=1}^M i \left( f_- \left( \frac{m-M+i}{n} \right) - \hat{f}_- \left( \frac{m-M+i}{n} \right) \right) \right| &< \frac{1}{d_M} \sum_{i=1}^M i \frac{c(2M+1)}{30n} \\ &= \frac{6}{M(M+1)(2M+1)} \frac{c(2M+1)}{30n} \frac{M(M+1)}{2} = \frac{c}{10n}. \end{aligned}$$

Thus, it holds

$$\mathcal{A} \subset \left\{ K_m < \frac{c}{5n} \text{ for } m < n\tau_0 \text{ and } K_m \geq \frac{4c}{5n} \text{ for } m = \lceil n\tau_0 \rceil + 3N - 1 \right\} \subset \{n\tau_0 \leq n\hat{\tau}_{K,n} \leq n\tau_0 + 3N\}$$

and therefore under the event  $\mathcal{A}$

$$0 \leq \hat{\tau}_{K,n} - \tau_0 \leq \frac{3N}{n}. \quad (14)$$

Now we can use (8) to get

$$\mathbb{P}_{\tau_0} \left( \max_{k < m \leq n} |Z_m| \geq \sqrt{8 \log n} \right) \leq n \exp \{-4 \log n\} = n^{-3}. \quad (15)$$

With the inequality (10) it follows that

$$\begin{aligned} & \mathbb{P}_{\tau_0} \left( \max_{1 \leq i \leq n} \left| f_- \left( \frac{i}{n} \right) - \hat{f}_- \left( \frac{i}{n} \right) \right| \geq \frac{c(2N+1)}{10n} \right) \\ & \leq \exp \left\{ -\frac{c^2(2N+1)^2(c^2n^2-cn)}{100n^2(8cn+4)} \right\} + \exp \left\{ -\frac{c^2(2N+1)^2(c^3n^2-c)}{9600n^3} \right\}, \\ & \asymp \exp \left\{ -n^{1/3} \log^{2/3} n \right\} \ll n^{-3}. \end{aligned}$$

Thus, it holds

$$\mathbb{P}_{\tau_0}(\mathcal{A}^c) \leq \mathbb{P}_{\tau_0} \left( \max_{1 \leq m \leq M} |Z_m| \geq \sqrt{8 \log M} \right) + \mathbb{P}_{\tau_0} \left( \max_{1 \leq i \leq n} \left| f_- \left( \frac{i}{n} \right) - \hat{f}_- \left( \frac{i}{n} \right) \right| \geq \frac{c(2N+1)}{10n} \right) \leq n^{-3}.$$

Based on this and (14), we get

$$\begin{aligned} & \max_{\theta_0 \in \Theta^K} \mathbb{E}_{\tau_0} \left[ \left( \frac{n^{1/3}}{\log^{1/3} n} (\tau_{K,n} - \tau_0) \right)^2 \right] \\ & = \max_{\theta_0 \in \Theta^K} \left( \mathbb{E}_{\tau_0} \left[ \left( \frac{n^{1/3}}{\log^{1/3} n} (\tau_{K,n} - \tau_0) \right)^2 \mathbb{I}(\mathcal{A}) \right] + \mathbb{E}_{\tau_0} \left[ \left( \frac{n^{1/3}}{\log^{1/3} n} (\tau_{K,n} - \tau_0) \right)^2 \mathbb{I}(\mathcal{A}^c) \right] \right) \\ & \leq \max_{\theta_0 \in \Theta} \left( \mathbb{E}_{\tau_0} \left[ \left( \frac{3N}{n^{2/3} \log^{1/3} n} \right)^2 \mathbb{I}(\mathcal{A}) \right] + \mathbb{E}_{\tau_0} \left[ \left( \frac{n^{1/3}}{\log^{1/3} n} \right)^2 \mathbb{I}(\mathcal{A}^c) \right] \right) \\ & \leq \left( \frac{3N}{n^{2/3} \log^{1/3} n} \right)^2 + \left( \frac{n^{1/3}}{\log^{1/3} n} \right)^2 n^{-3} \leq 9b^2 + 1 = 9 \cdot \left( \frac{300}{c^2} \right)^{2/3} + 1, \end{aligned}$$

using the inequality  $1/\log^{2/3} n \leq 1$  for  $n > 2$ . Thus, the statement for a kink is true with  $r_K^* = 9(300/\delta_0^2)^{2/3} + 1$ .  $\square$

*Proof of Theorem 3.* We are going to prove the statement by contradiction. The proof follows a similar structure to that of Theorem 6.12 in Korostelev and Korosteleva (2011), which establishes the result for the special case of a jump and  $\beta_- = \beta_+ = 0$ . The initial steps are identical for the cases of a kink and a jump. Let  $\psi_n$  be a sequence satisfying  $\frac{1}{n} \leq \psi_n \ll 1$ .

We fix  $\alpha_- = \beta_- = 0$  and some  $\alpha_+$  and  $\beta_+$ , because a lower rate obtained over the fixed parameters is also a lower rate for the whole parameter space. We set  $M := \lfloor (1 - 2\delta_0)/3b\psi_n \rfloor$ , with  $b$  a positive constant independent of  $n$ , to be determined later. We choose  $t_0, \dots, t_M \in (\delta_0, 1 - \delta_0)$  such that  $t_j - t_{j-1} = 3b\psi_n$  for  $j = 0, \dots, M$  and  $M > 1$ . As  $\frac{1}{n} \leq \psi_n \ll 1$ , this is possible. Now we assume that

$$\liminf_{n \rightarrow \infty} \inf_{\tilde{\tau}_n \in \mathcal{T}} \max_{\tau_0 \in (\delta_0, 1 - \delta_0)} \mathbb{E}_{\tau_0} \left[ \left( \frac{\hat{\tau}_n - \tau_0}{\psi_n} \right)^2 \right] = 0.$$

Then, there exists a family of Markov stopping times  $(\tilde{\tau}_n)_{n \in \mathbb{N}}$  such that

$$\lim_{n \rightarrow \infty} \max_{0 \leq j \leq M} \mathbb{E}_{t_j} \left[ \left( \frac{\tilde{\tau}_n - t_j}{\psi_n} \right)^2 \right] = 0. \quad (16)$$

By Markov's inequality, we have

$$\mathbb{P}_{t_j} (|\tilde{\tau}_n - t_j| > b\psi_n) \leq \frac{\mathbb{E}_{t_j} [|\tilde{\tau}_n - t_j|^2]}{(b\psi_n)^2},$$

and further, by (16),

$$\lim_{n \rightarrow \infty} \max_{0 \leq j \leq M} \mathbb{P}_{t_j} (|\tilde{\tau}_n - t_j| > b\psi_n) = 0.$$

Hence, for  $n$  large enough,

$$\max_{0 \leq j \leq M} \mathbb{P}_{t_j} (|\tilde{\tau}_n - t_j| > b\psi_n) \leq \frac{1}{4}. \quad (17)$$

Let  $\mathcal{B}_j := \{|\tilde{\tau}_n - t_j| \leq b\psi_n\}$ . The distance between two distinct points of  $t_0, \dots, t_M$  is always greater than  $3b\psi_n$ , so the events  $\mathcal{B}_j$  are all mutually exclusive. Note also that  $\bigcup_{j=0}^{M-1} \mathcal{B}_j \subset \{|\tilde{\tau} - t_M| > b\psi_n\}$ . We denote

$$\mathbf{d}\mathbb{P}_{t_j} = \frac{1}{(\sqrt{2\pi})^n} \prod_{i=1}^n \exp \left\{ -\frac{1}{2} (X_i - f_{t_j})^2 \right\},$$

the likelihood function of  $X_1, \dots, X_n$  under the change point  $t_j$ . Next we can calculate

$$\begin{aligned} \sum_{j=0}^{M-1} \mathbb{E}_{t_j} \left[ \frac{\mathbf{d}\mathbb{P}_{t_M} \mathbb{I}(\mathcal{B}_j)}{\mathbf{d}\mathbb{P}_{t_j}} \right] &= \sum_{j=0}^{M-1} \mathbb{E}_{t_M} [\mathbb{I}(\mathcal{B}_j)] = \sum_{j=0}^{M-1} \mathbb{P}_{t_M}(\mathcal{B}_j) = \mathbb{P}_{t_M} \left( \bigcup_{j=0}^{M-1} \mathcal{B}_j \right) \\ &\leq \mathbb{P}_{t_M} (|\tilde{\tau}_n - t_M| > b\psi_n) \leq \max_{0 \leq j \leq M} \mathbb{P}_{t_j} (|\tilde{\tau}_n - t_j| > b\psi_n). \end{aligned}$$

And by (17), we have, for  $n$  large enough,

$$\sum_{j=0}^{M-1} \mathbb{E}_{t_j} \left[ \frac{\mathbf{d}\mathbb{P}_{t_M} \mathbb{I}(\mathcal{B}_j)}{\mathbf{d}\mathbb{P}_{t_j}} \right] \leq \frac{1}{4}. \quad (18)$$

Now we can calculate the likelihood ratio. For notational convenience, we write  $f_j(i) := f_{t_j}(i/n)$  and  $f_M(i) := f_{t_M}(i/n)$ . Note that  $f_j(i) = 0 = f_M(i)$  for  $i \leq t_j < t_M$ . Then

$$\begin{aligned} \frac{\mathbf{d}\mathbb{P}_{t_M}}{\mathbf{d}\mathbb{P}_{t_j}} &= \frac{\prod_{i=1}^n \exp \left\{ -\frac{1}{2} (X_i - f_M(i))^2 \right\}}{\prod_{i=1}^n \exp \left\{ -\frac{1}{2} (X_i - f_j(i))^2 \right\}} \\ &= \exp \left\{ \sum_{i=\lfloor t_j n \rfloor + 1}^n \frac{1}{2} \left( (X_i - f_j(i))^2 - (X_i - f_M(i))^2 \right) \right\}, \end{aligned}$$

and

$$\begin{aligned} \frac{1}{2} \left( (X_i - f_j(i))^2 - (X_i - f_M(i))^2 \right) &= \frac{1}{2} (2X_i (f_M(i) - f_j(i)) + f_j^2(i) - f_M^2(i)) \\ &= \varepsilon_i (f_M(i) - f_j(i)) - \frac{1}{2} (f_M(i) - f_j(i))^2, \end{aligned}$$

where  $\varepsilon_i = X_i - f_j(i) \sim \mathcal{N}(0, 1)$  if  $(X_i)_{i=1}^n \sim \mathbb{P}_{t_j}$ . Now we can use the moment generating function of the standard normal,  $\mathbb{E}[\exp\{tZ\}] = \exp\{\frac{1}{2}t^2\}$ , to get

$$\mathbb{E}_{t_j} \left[ \exp \left\{ \varepsilon_i (f_M(i) - f_j(i)) - \frac{1}{2} (f_M(i) - f_j(i))^2 \right\} \right] = 1. \quad (19)$$

We set  $u_j := t_j + b\psi_n$ . Note that  $f_M(i) = 0$  for  $i \leq u_j < t_M$ . We define  $g_n$  as

$$g_n := \sum_{i=[t_j n]+1}^{[u_j n]} \frac{1}{2} (f_M(i) - f_j(i))^2 = \frac{1}{2} \sum_{i=[t_j n]+1}^{[u_j n]} \left( \beta_+ \left( \frac{i}{n} - t_j \right) + \alpha_+ \right)^2 = \frac{1}{2} \sum_{i=1}^{[b\psi_n n]} \left( \beta_+ \frac{i}{n} + \alpha_+ \right)^2.$$

Note that  $g_n$  is not dependent on  $j$ .

Next we define  $Z_j$  as

$$Z_j := \left( - \sum_{i=[t_j n]+1}^{[u_j n]} \varepsilon_i f_j(i) \right) / \sqrt{\sum_{i=[t_j n]+1}^{[u_j n]} f_j(i)^2} \sim \mathcal{N}(0, 1).$$

Since  $\tilde{\tau}$  is a Markov stopping time, the event  $\mathcal{B}_j = \{|\tilde{\tau} - t_j| \leq b\psi_n\}$  is  $\mathcal{F}_{u_j}$ -measurable and is therefore independent of  $X_i$  and  $\varepsilon_i$ , for  $i = [u_j n] + 1, \dots, n$ . We can use this independence and (19), to rewrite the sum in (18) as

$$\begin{aligned} \mathbb{E}_{t_j} \left[ \frac{d\mathbb{P}_{t_M}}{d\mathbb{P}_{t_j}} \mathbb{I}(\mathcal{B}_j) \right] &= \mathbb{E}_{t_j} \left[ \exp \left\{ \sum_{i=[t_j n]+1}^n \varepsilon_i (f_M(i) - f_j(i)) - \frac{1}{2} (f_M(i) - f_j(i))^2 \right\} \mathbb{I}(\mathcal{B}_j) \right] \\ &= \mathbb{E}_{t_j} \left[ \exp \left\{ \sum_{i=[t_j n]+1}^{[u_j n]} \varepsilon_i (f_M(i) - f_j(i)) - \sum_{i=[t_j n]+1}^{[u_j n]} \frac{1}{2} (f_M(i) - f_j(i))^2 \right\} \mathbb{I}(\mathcal{B}_j) \right] \\ &\quad \cdot \prod_{i=[u_j n]+1}^n \mathbb{E}_{t_j} \left[ \exp \left\{ \varepsilon_i (f_M(i) - f_j(i)) - \frac{1}{2} (f_M(i) - f_j(i))^2 \right\} \right] \\ &= \mathbb{E}_{t_j} \left[ \exp \left\{ \left( - \sum_{i=[t_j n]+1}^{[u_j n]} \varepsilon_i f_j(i) \right) - g_n \right\} \mathbb{I}(\mathcal{B}_j) \right] \\ &= \mathbb{E}_{t_j} \left[ \exp \left\{ \sqrt{\sum_{i=[t_j n]+1}^{[u_j n]} (f_j(i))^2} Z_j - g_n \right\} \mathbb{I}(\mathcal{B}_j) \right] \\ &\geq \mathbb{E}_{t_j} \left[ \exp \left\{ \sqrt{\sum_{i=[t_j n]+1}^{[u_j n]} (f_j(i))^2} Z_j - g_n \right\} \mathbb{I}(\mathcal{B}_j) \mathbb{I}(Z_j \geq 0) \right] \\ &\geq \exp \{-g_n\} \mathbb{P}_{t_j}(\mathcal{B}_j \cap \{Z_j \geq 0\}). \end{aligned}$$

Because of (17), it holds that  $\mathbb{P}_{t_j}(\mathcal{B}_j) \geq 3/4$ . Then

$$\begin{aligned} \mathbb{P}(\mathcal{B}_j \cap \{Z_j \geq 0\}) &= \mathbb{P}(\mathcal{B}_j) + \mathbb{P}(Z_j \geq 0) - \mathbb{P}_{t_j}(\mathcal{B}_j \cup \{Z_j \geq 0\}) \\ &\geq \frac{3}{4} + \frac{1}{2} - 1 = \frac{1}{4}. \end{aligned}$$

Combining this with (18), we get

$$\frac{1}{4} \geq \frac{1}{4} \sum_{j=0}^{M-1} \exp \{-g_n\} = \frac{M}{4} \exp \{-g_n\} = \left\lfloor \frac{(1-2\delta_0)}{3b\psi_n} \right\rfloor \frac{1}{4} \exp \{-g_n\} \asymp \frac{\exp \{-g_n\}}{\psi_n}. \quad (20)$$

**For a jump** For a jump, we can set  $\beta_+ = 0$ ,  $|\alpha_+| \geq \delta_0$  and  $\psi_n = \log n/n$ . Then

$$g_n = \frac{1}{2} \sum_{i=1}^{b \log n} \alpha_+^2 = \frac{\alpha_+^2 b}{2} \log n.$$

With  $b = \alpha_+^{-2}$ , it holds that

$$\frac{n}{\log n} \exp \left\{ -\frac{\alpha_+^2 b}{2} \log n \right\} = \frac{n}{\log n} \exp \left\{ -\frac{1}{2} \log n \right\} = \frac{\sqrt{n}}{\log n} \rightarrow \infty, \text{ for } n \rightarrow \infty.$$

Thus,  $\frac{n}{\log n} \exp \{-g_n\} \rightarrow \infty$  for  $n \rightarrow \infty$ , which is a contradiction to (20), so the statement is true.

**For a kink** Now we set  $\alpha_+ = 0$ ,  $|\beta_+| \geq \delta_0$  and  $\psi_n = n^{1/3} / \log^{1/3} n$ . Then, it holds

$$\begin{aligned} g_n &= \frac{1}{2} \sum_{i=1}^{bn^{2/3} \log^{1/3} n} \left( \beta_+ \frac{i}{n} \right)^2 = \frac{\beta_+^2}{12n^2} (2b^3 n^2 \log n + 3b^2 n^{4/3} \log^{2/3} n + bn^{2/3} \log^{1/3} n) \\ &= \frac{\beta_+^2 b^3 \log n}{6} + \frac{\beta_+^2 b^2 \log^{2/3} n}{4n^{2/3}} + \frac{\beta_+^2 b \log^{1/3} n}{12n^{4/3}}. \end{aligned}$$

For  $b = \beta_+^{-2/3}$ , we get

$$\exp \left\{ -\frac{\beta_+^2 b^2 \log^{2/3} n}{4n^{2/3}} - \frac{\beta_+^2 b \log^{1/3} n}{12n^{4/3}} \right\} \rightarrow 1, \text{ for } n \rightarrow \infty,$$

and

$$\frac{n^{1/3}}{\log^{1/3} n} \exp \left\{ -\frac{\beta_+^2 b^3 \log n}{6} \right\} = \frac{n^{1/3}}{\log^{1/3} n} \exp \left\{ -\frac{1}{6} \log n \right\} = \frac{n^{1/6}}{\log^{1/3} n} \rightarrow \infty, \text{ for } n \rightarrow \infty.$$

Thus,  $(n^{1/3} / \log^{1/3}) \exp \{-g_n\} \rightarrow \infty$ , for  $n \rightarrow \infty$ , which is a contradiction to (20).  $\square$

## 6 Discussion

We have studied the online detection of changes in segmented linear models with additive i.i.d. Gaussian noise. Our focus is on the minimax rate optimality in estimating the change point as well as computational and memory efficiency. We introduce the online detector FLOC, which offers several practical advantages, including ease of implementation as well as constant computational and memory complexity for every newly incoming data point — crucial attributes for effective online algorithms. From a statistical perspective, FLOC achieves minimax optimal rates for detecting changes in both function values (i.e. jump) and slopes (i.e. kink). We believe that this is of particular practical benefit, as in many applications the type of change is not always clear beforehand. Notably, our results reveal a phase transition between the jump and kink scenarios, which echo the understanding in the offline setup (Goldenshluger et al., 2006, Frick et al., 2014b, Chen, 2021; see also Table 1). The FLOC detector is specifically designed to achieve asymptotically minimax optimal rates. While the constants involved have not been fully optimized and could likely be improved, we preliminary guidance for tuning FLOC to improve its empirical performance in finite-sample settings. Alternative approaches for parameter tuning could further enhance the performance of FLOC. For instance, theoretical insights, such as the limiting distribution of detection delay provided by Aue et al. (2009), could guide the selection of thresholds to satisfy specified bounds on type II error, and bootstrapping methods, as introduced by Hušková and Kirch (2012), could be adapted to improve performance, particularly in small-sample scenarios. The current implementation of FLOC relies on sufficient historical data to accurately estimate the pre-change signal. As a practical extension, an adaptive approach could be developed to incrementally update the signal estimate as new observations become available.

Monitoring simultaneously jumps and kinks can enhance detection power compared to conventional approaches that focus solely on mean changes, as demonstrated in our analysis of excess mortality data. However, practitioners should be aware that the Gaussian noise and linear signal assumptions may be strongly violated in certain real-world applications. Enhancing the robustness of FLOC to accommodate broader noise distributions and signal structures, represents a promising direction for future research. For example, in the application

discussed in Section 4.3, it is interesting to develop a refined analysis by incorporating serial dependencies. Finally, from a theoretical perspective, the extension of minimax rate results to more general settings, such as piecewise polynomial signals or changes in higher-order derivatives, remains an open problem and is worth further investigation.

## Acknowledgements

The authors gratefully acknowledge support from the Deutsche Forschungsgemeinschaft (DFG, German Research Foundation) under Germany’s Excellence Strategy–EXC 2067/1-390729940. HL and AM further acknowledge funding from the DFG Collaborative Research Center 1456. AM additionally acknowledges support from the DFG Research Unit 5381.

## References

- Amiri, A. and Allahyari, S. (2012). Change point estimation methods for control chart postsignal diagnostics: a literature review. *Qual. Reliab. Eng. Int.*, 28(7):673–685.
- Anscombe, F. J. (1946). Linear sequential rectifying inspection for controlling fraction defective. *Suppl. J. Roy. Statist. Soc.*, 8:216–222.
- Aue, A. and Horváth, L. (2004). Delay time in sequential detection of change. *Statist. Probab. Lett.*, 67(3):221–231.
- Aue, A., Horváth, L., and Reimherr, M. L. (2009). Delay times of sequential procedures for multiple time series regression models. *J. Econometrics*, 149(2):174–190.
- Bai, J. and Perron, P. (1998). Estimating and testing linear models with multiple structural changes. *Econometrica*, 66(1):47–78.
- Chan, H. P. (2017). Optimal sequential detection in multi-stream data. *Ann. Statist.*, 45(6):2736–2763.
- Chen, H. (2019). Sequential change-point detection based on nearest neighbors. *Ann. Statist.*, 47(3):1381–1407.
- Chen, Y. (2021). Jump or kink: on super-efficiency in segmented linear regression breakpoint estimation. *Biometrika*, 108(1):215–222.
- Chen, Y., Wang, T., and Samworth, R. J. (2022). High-dimensional, multiscale online changepoint detection. *J. R. Stat. Soc. Ser. B. Stat. Methodol.*, 84(1):234–266.
- Chen, Y., Wang, T., and Samworth, R. J. (2024). Inference in high-dimensional online changepoint detection. *J. Amer. Statist. Assoc.*, 119(546):1461–1472.
- Cho, H. and Kirch, C. (2024). Data segmentation algorithms: univariate mean change and beyond. *Econom. Stat.*, 30:76–95.
- Cho, H., Kley, T., and Li, H. (2024). Detection and inference of changes in high-dimensional linear regression with non-sparse structures. *arXiv preprint arXiv:2402.06915v3*.
- Detle, H., Munk, A., and Wagner, T. (1998). Estimating the variance in nonparametric regression—what is a reasonable choice? *J. R. Stat. Soc. Ser. B. Stat. Methodol.*, 60(4):751–764.
- Frick, K., Munk, A., and Sieling, H. (2014a). Multiscale change point inference. *J. R. Stat. Soc. Ser. B. Stat. Methodol.*, 76(3):495–580. With 32 discussions by 47 authors and a rejoinder by the authors.

- Frick, S., Hohage, T., and Munk, A. (2014b). Asymptotic laws for change point estimation in inverse regression. *Statist. Sinica*, 24(2):555–575.
- Goldenshluger, A., Tsybakov, A., and Zeevi, A. (2006). Optimal change-point estimation from indirect observations. *Ann. Statist.*, 34(1):350–372.
- Hall, P. and Marron, J. S. (1990). On variance estimation in nonparametric regression. *Biometrika*, 77(2):415–419.
- Horváth, L., Kokoszka, P., and Wang, S. (2021). Monitoring for a change point in a sequence of distributions. *Ann. Statist.*, 49(4):2271–2291.
- Hušková, M. and Kirch, C. (2012). Bootstrapping sequential change-point tests for linear regression. *Metrika*, 75(5):673–708.
- Korostelev, A. and Korosteleva, O. (2011). *Mathematical Statistics: Asymptotic Minimax Theory*. American Mathematical Society.
- Kovács, S., Bühlmann, P., Li, H., and Munk, A. (2023). Seeded binary segmentation: a general methodology for fast and optimal changepoint detection. *Biometrika*, 110(1):249–256.
- Kovács, S., Li, H., Haubner, L., Munk, A., and Bühlmann, P. (2024). Optimistic search: Change point estimation for large-scale data via adaptive logarithmic queries. *J. Mach. Learn. Res.*, 25(297):1–64.
- Lai, T. L. (2001). Sequential analysis: some classical problems and new challenges. *Statist. Sinica*, 11(2):303–408. With comments and a rejoinder by the author.
- Lee, S., Seo, M. H., and Shin, Y. (2016). The lasso for high dimensional regression with a possible change point. *J. R. Stat. Soc. Ser. B. Stat. Methodol.*, 78(1):193–210.
- Li, Z., Peng, Z., Hollis, D., Zhu, L., and McClellan, J. (2018). High-resolution seismic event detection using local similarity for Large-N arrays. *Sci. Rep.*, 8(1):1646.
- Lorden, G. (1971). Procedures for reacting to a change in distribution. *Ann. Math. Statist.*, 42:1897–1908.
- Muggeo, V. M. (2003). Estimating regression models with unknown break-points. *Stat. Med.*, 22(19):3055–3071.
- Niu, Y. S., Hao, N., and Zhang, H. (2016). Multiple change-point detection: A selective overview. *Statist. Sci.*, 31(4):611–623.
- Noufaily, A., Enki, D. G., Farrington, P., Garthwaite, P., Andrews, N., and Charlett, A. (2013). An improved algorithm for outbreak detection in multiple surveillance systems. *Stat. Med.*, 32(7):1206–1222.
- Page, E. S. (1954). Continuous inspection schemes. *Biometrika*, 41:100–115.
- Pollak, M. (1985). Optimal detection of a change in distribution. *Ann. Statist.*, 13(1):206–227.
- Polunchenko, A. S. and Tartakovsky, A. G. (2010). On optimality of the Shiryaev-Roberts procedure for detecting a change in distribution. *Ann. Statist.*, 38(6):3445–3457.
- Roberts, S. W. (1966). A comparison of some control chart procedures. *Technometrics*, 8:411–430.
- Romano, G., Eckley, I. A., and Fearnhead, P. (2024). A log-linear nonparametric online changepoint detection algorithm based on functional pruning. *IEEE Trans. Signal Process.*, 72:594–606.
- Romano, G., Eckley, I. A., Fearnhead, P., and Rigai, G. (2023). Fast online changepoint detection via functional pruning CUSUM statistics. *J. Mach. Learn. Res.*, 24(81):1–36.
- Shewhart, W. (1931). *Economic Control of Quality of Manufactured Product*. Van Nostrand Co., New York.

- Shiryaev, A. N. (1961). The problem of the most rapid detection of a disturbance in a stationary process. In *Soviet Math. Dokl.*, volume 2, page 103.
- Shiryaev, A. N. (1963). On optimum methods in quickest detection problems. *Theory Probab. Appl.*, 8(1):22–46.
- Siegmund, D. (1985). *Sequential Analysis: Tests and Confidence Intervals*. Springer Series in Statistics. Springer-Verlag, New York.
- Tartakovsky, A. G. (2020). *Sequential change detection and hypothesis testing—general non-i.i.d. stochastic models and asymptotically optimal rules*, volume 165 of *Monographs on Statistics and Applied Probability*. CRC Press, Boca Raton, FL.
- Tartakovsky, A. G., Polunchenko, A. S., and Sokolov, G. (2012). Efficient computer network anomaly detection by changepoint detection methods. *IEEE J. Sel. Top. Signal Process.*, 7(1):4–11.
- Truong, C., Oudre, L., and Vayatis, N. (2020). Selective review of offline change point detection methods. *Signal Process.*, 167:1–20.
- Wald, A. (1945). Sequential tests of statistical hypotheses. *Ann. Math. Statistics*, 16:117–186.
- Wang, H. and Xie, Y. (2024). Sequential change-point detection: Computation versus statistical performance. *Wiley Interdiscip. Rev. Comput. Stat.*, 16(1):1–22.
- Ward, K., Romano, G., Eckley, I., and Fearnhead, P. (2024). A constant-per-iteration likelihood ratio test for online changepoint detection for exponential family models. *Stat. Comput.*, 34(99):1–11.
- Yakir, B., Krieger, A. M., and Pollak, M. (1999). Detecting a change in regression: First-order optimality. *Ann. Statist.*, 27(6):1896–1913.
- Yao, Q. W. (1993). Asymptotically optimal detection of a change in a linear model. *Sequential Anal.*, 12(3-4):201–210.
- Yu, Y., Madrid Padilla, O. H., Wang, D., and Rinaldo, A. (2023). A note on online change point detection. *Sequential Anal.*, 42(4):438–471.